J. Physiol. (1979), **295**, 283–305
With 14 text-figures
Printed in Great Britain

DIFFERENTIAL CONDUCTION BLOCK IN BRANCHES OF A BIFURCATING AXON

BY Y. GROSSMAN*, I. PARNAS AND M. E. SPIRA
From the Neurobiology Unit, Institute of Life Sciences, the Hebrew University, Jerusalem, Israel

(*Received 4 August 1978*)

SUMMARY

1. Propagation of action potentials at high frequency was studied in a branching axon of the lobster by means of simultaneous intracellular recording both before and after the branch point.

2. Although the branching axon studied has a geometrical ratio close to one (perfect impedance matching) conduction across the branch point failed at stimulation frequencies above 30 Hz.

3. The block of conduction after high frequency stimulation occurred at the branch point *per se*. The parent axon and daughter branches continued to conduct action potentials.

4. Conduction block after high frequency stimulation appeared first in the thicker daughter branch and only later in the thin branch.

5. With high frequency stimulation there was a 10–15 % reduction in amplitude of the action potential in the parent axon, a corresponding decrease in the rate of rise of the action potential, a 25–30 % decrease in conduction velocity, marked increase in threshold and prolongation of the refractory period. In addition the membrane was depolarized by 1–3 mV.

6. Measurements of the membrane current using the patch clamp technique showed a large decrease in the phase of inward current associated with the action potential, before the branching point.

7. The small membrane depolarization seen after high frequency stimulation is not the sole cause of the conduction block. Imposed prolonged membrane depolarization (8 mV for 120 sec) was insufficient to produce conduction block.

8. *In vivo* chronic extracellular recordings from the main nerve bundle (which contains the parent axon) and the large daughter branch revealed that: (*a*) the duration and frequency of trains of action potentials along the axons exceeded those used in the isolated nerve experiments and (*b*) conduction failure in the large daughter branch could be induced in the whole animal by electrical stimulation of the main branch as in the isolated preparation.

9. Possible mechanisms underlying block of conduction after high frequency stimulation in a branching axon are discussed.

* Present address: Unit of Comparative Medicine, Faculty of Health Sciences, Ben Gurion University, Beer-Sheva, Israel.

0022-3751/79/5110-0670 $01.50

INTRODUCTION

It has been shown both experimentally and theoretically that a train or 'code' of action potentials is not always transmitted faithfully along an axon or its daughter branches. Depending on the geometry of the axon, the periaxonal space, the membrane properties or frequency of the action potentials, conduction can be altered or even blocked at certain regions along the axon. The structure of the axon at such regions shows a step or a gradual increase in diameter (Waxman, 1972, 1975; Khodorov, Timin, Vilenkin & Gul'ko, 1969; Khodorov, Timin, Posin & Shemelev, 1971; Spira, Yarom & Parnas, 1976; Parnas, Hochstein & Parnas, 1976), a bifurcation (Parnas, 1972; Grossman, Spira & Parnas, 1973; Goldstein & Rall, 1974; Van Essen, 1973; Yau, 1976), or a thick layer of enveloping sheaths which apparently restricts diffusion (Hatt & Smith, 1975, 1976). Such inhomogeneities in axonal structure may, but not always, produce regions of a low safety factor and thus trains of impulses are transmitted at low but not at high frequencies.

Several mechanisms have been suggested to explain differential conduction of action potential trains in branches of the same axon. These include differential maximal sodium conductances per cm^2 for each branch (Chung, Raymond & Lettvin, 1970; Zeevi, 1972), membrane hyperpolarization by the activation of an electrogenic Na pump (Jansen & Nicholls, 1973; Van Essen, 1973) and accumulation of K in the extracellular space to produce membrane depolarization and Na inactivation (Spira *et al.* 1976).

The common excitatory and inhibitory axons innervating the medial and lateral bundles of the deep abdominal extensor muscles of the lobster (Parnas & Atwood, 1966) are favourable preparations for the study of the mechanisms involved in the block of action potential conduction at points of bifurcation. When the common excitatory axon is stimulated at a low frequency (below 15 Hz), excitatory synaptic potentials and action potentials could be recorded only from the medial muscle fibres. Between 14 and 50 Hz the two muscles responded; however, above 50 Hz conduction of the action potentials was rapidly blocked in the medial bundle branch while it continued for many seconds in the lateral branch, even at a considerably higher frequency of stimulation (Parnas, 1972).

The common excitatory axon innervating the medial and lateral muscle bundles is relatively large (50–75 μm), enabling intracellular recording from points before and after the main bifurcation to the two muscles. Thus, it was possible to show that the conduction block of high frequency trains of action potentials into the medial branch occurred at the main bifurcation of the axon (Grossman *et al.* 1973).

In the present and the following article, we used the common excitatory axon to study in more detail the changes occurring in conduction of action potentials during high frequency activation. Mechanisms enabling such a differential block of action potential conduction and the effects of changes of K and Ca concentration are explored (Grossman, Parnas & Spira, 1979). In a third article (Parnas & Segev, 1979), a theoretical model describing propagation of trains of action potentials in a bifurcating axon is given.

METHODS

Animals. The spiny lobster, *Panulirus penicillatus* was used. Animals collected at the Gulf of Eilat were kept in aquaria with constantly filtered running sea water at 18–20 °C.

Preparation. The anatomical organization of the deep abdominal extensor muscles (medial and lateral) and their pattern of innervation is given by Parnas & Atwood (1966). The nerve innervating the deep extensor muscles was exposed after removing the flexor muscles. The nerve bundle

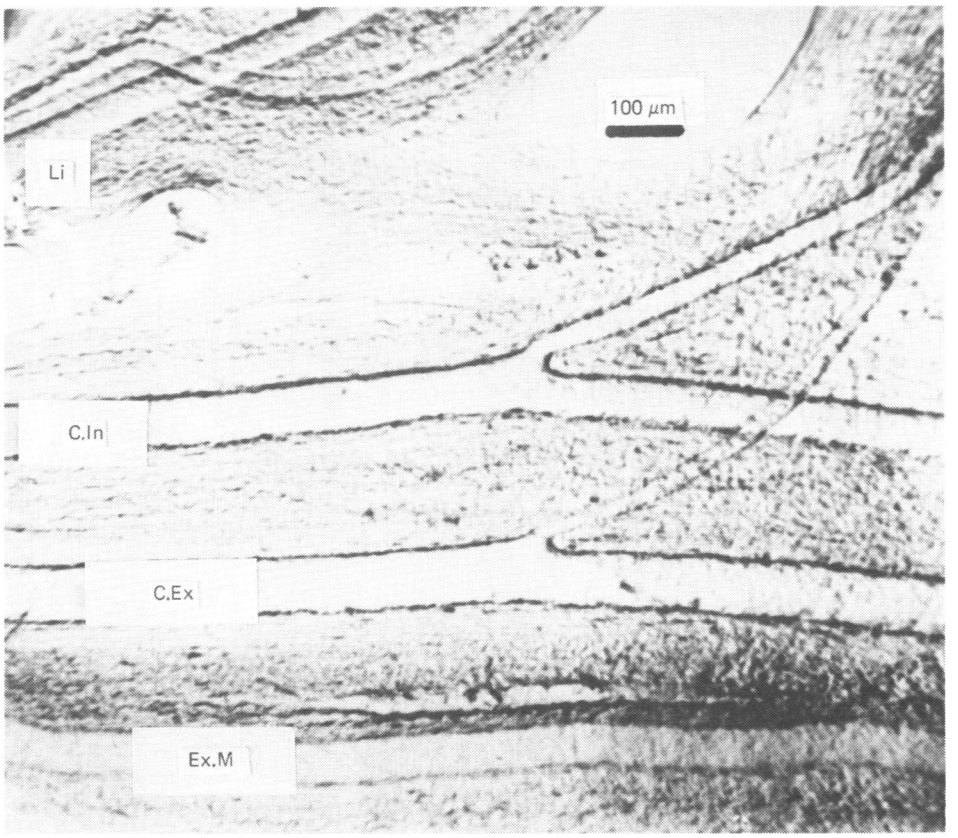

Fig. 1. Axons in the nerve bundle innervating the medial and lateral bundles of the deep abdominal muscles. Li, excitor axon to the lateral bundle. C.In, common inhibitor. C.Ex, common excitor. Ex.M, specific excitor to the medical bundle.

including its two main branches (to the medial and lateral) was carefully excised and pinned in a chamber containing Sylgard resin. A region of an isolated bundle including the axons innervating both branches is shown in Fig. 1. Identification of the axons was achieved in some experiments by keeping the nerve-muscle connexions intact and stimulating each axon intracellularly while recording (also intracellularly) the responses of the muscles. The axons in different preparations, which were taken from the abdominal segments 2–4, appeared always to have the same spatial relationship. The largest axon is the common excitor (axon 2 of Parnas & Atwood, 1966). The second in size is the common inhibitor (axon 5) and the smallest is the medial (axon 1). Dissection and experiments were made under a constant flow of physiological solution at 20–22 °C.

Solution. The physiological solution was based on an analysis of the haemolymph of *Panulirus penicillatus*. The concentrations of Na^+ and K^+ were determined by flame photometry and that of Na^+, K^+, Mg^+ and Ca^{2+} by atomic absorption spectrophotometry (Perkin Elmer 290). Among the anions only chloride was determined using a Radiometer titrator (CMT 10). Osmolarity was

measured kryoscopically (Halbmicro Osmometer, Knawer). Ninety-eight per cent of the cations were found to be present as chloride salts. The physiological solution used was NaCl 520 mM, KCl 12 mM, $MgCl_2$ 10 mM, $CaCl_2$ 12 mM, Tris chloride 2·5 mM. The pH was adjusted to 7·4. In this physiological solution the preparation survived well, showing constant membrane potential and action potential amplitude for several hours.

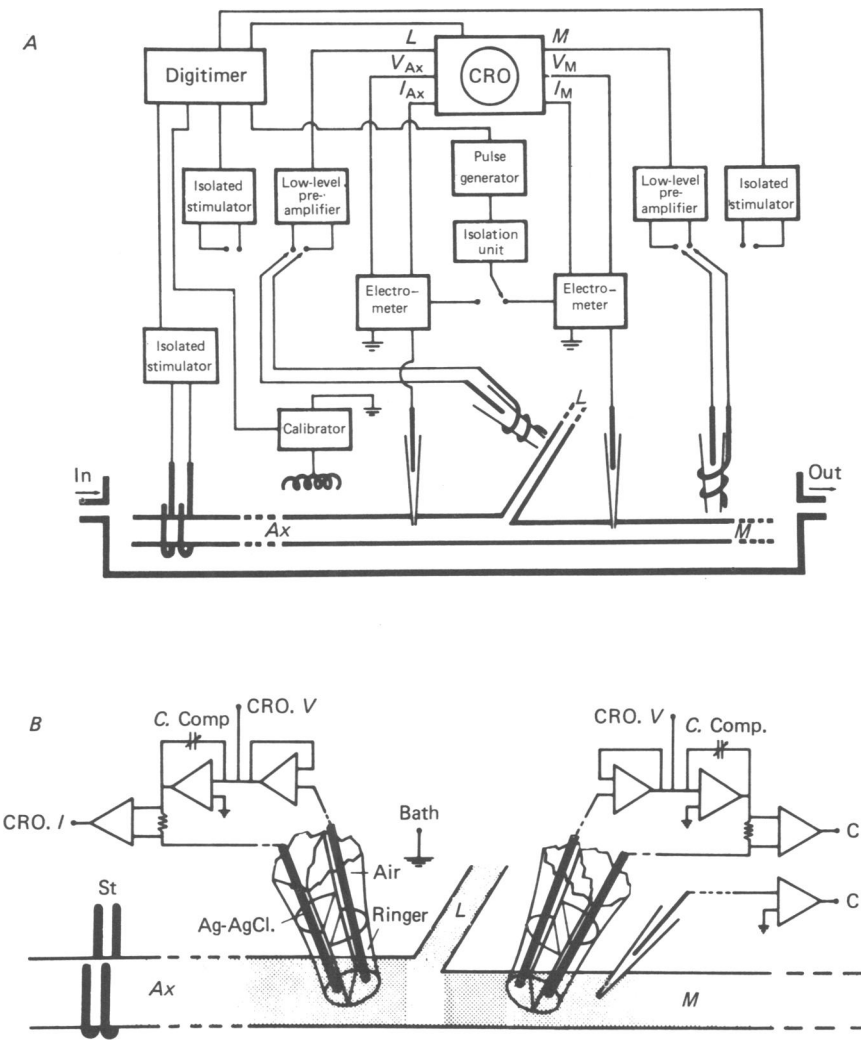

Fig. 2. *A*, experimental setup. *B*, patch clamp system to measure membrane current. *Ax*, *M* and *L* the main and daughter axonal branches. St, stimulating electrodes. Suction electrodes and micro-electrodes recorded action potentials at *M*, *L* and *Ax*.

Stimulation and recording. Extracellular recording and stimulation were achieved with either Ag-AgCl hook electrodes or suction electrodes. Each electrode could be used for stimulation and recording. For recording, the electrodes were connected to Tektronix 122 low level pre-amplifiers. Devices Digitimer type 3290 stimulator with mark IV isolation units were used for stimulation.

For intracellular recording and stimulation, 10–20 MΩ, 2 M-KCl micro-electrodes were used. Recording techniques were as described previously (Spira *et al.* 1976).

Determination of space constant, I–V curves and membrane resistance. In order to determine the membrane properties, three micro-electrodes were inserted into an axon. Each electrode served

for recording and stimulation and thus the membrane voltage drop for an intracellular current pulse could be measured at three points. The space constant (λ) and membrane resistance (R_m) were determined by the method described by Papir (1973). Current–voltage curves were obtained either by injecting square current pulses of different intensities or by the injection of a ramp current pulse of 0·5 sec duration, which is long in comparison to the membrane time constant. The experimental set-up is diagrammatically shown in Fig. 2*A*.

Patch clamp experiments. Membrane currents were measured using the patch clamp technique (Frank & Tauc, 1963; Neher & Lux, 1969). Double barrel micro-electrodes were prepared from theta glass tubes. The tip was broken to the desired diameter (30–70 μm) and fire polished. The tips were immersed in physiological solution allowing the liquid to enter by capillary forces. The rest of the barrel was kept empty in order to minimize capacitative coupling. The resistance of each of the electrode barrels was between 20–50 kΩ. When pressed against the axon resistance increased to about 300–500 kΩ. The electrode potential was clamped to that of the bath electrode and the clamping current measured (for more details see diagram in Fig. 2*B*).

In vivo chronic recordings from nerves and muscles. The lobsters' body temperatures were lowered by keeping them on ice before and during the operation. A small window (5 × 10 mm) was opened in the cuticle at the dorsal surface of either the second or third abdominal segment. The deep extensor muscles and their nerves were gently exposed by removal of small pieces of the superficial extensor muscles. Fine (100 μm) silver wires, insulated except at their tips, were implanted into the muscle to record electromyograms. Hook electrodes (100μm) were placed around the medial nerve branch and around the main bundle before the bifurcation. In some experiments two electrode pairs were implanted around the main axon branch, the proximal serving for stimulation, the distal for recording. It was impossible to record directly from the small lateral nerve branch. The cuticle was then replaced and covered with dental cement. The electrodes were connected through low level Tektronix 122 preamplifiers to a 4-channel tape recorder (Hewlett Packard, model 3960). The animals were placed in a container (100 × 60 × 50 cm) with sea water and after about 0·5–1 hr of recovery showed swimming and escape responses. An animal could be used for chronic recording for several days after which the signals became weak or disappeared altogether. At this stage we usually found that connective tissue had grown over the electrodes.

RESULTS

Characterization of the experimental system. We will first describe the geometry of the axon and its membrane properties at rest. The diameters of the main axon (*Ax*) and its branches (*M* to medial and *L* to lateral) were measured in fresh preparations and from fixed cross-sections using an ocular with a micrometric graticule. The differences in the diameter of the axons as measured from fresh and fixed preparations did not exceed 10%. In twenty-two preparations the diameters of the different branches were: *Ax*, 75·1 ± 8·9 μm (mean ± S.D.); *M*, 64·8 ± 9·9 μm and *L*, 24·5 ± 2·7 μm. The geometrical ratio (*GR*) of Rall (1959, 1964)

$$GR = \frac{d_M^{3/2} + d_L^{3/2}}{d_{Ax}^{3/2}}$$

(where d_M, d_L and d_{Ax} are the diameters of *M*, *L* and *Ax* respectively) is one (0·97 ± 0·08). Assuming membrane homogeneity, this finding implies impedance matching between the main axon and daughter branches; therefore, an action potential should propagate from *Ax* into *L* and *M* with the same safety factor as into an equivalent axon with the same diameter as *Ax* (Goldstein & Rall, 1974; Parnas & Segev, 1979). In other words, single action potentials should propagate equally well into the *L* and *M* branches. Stimulation of the axon produced overshooting action potentials that propagated into the *M* and *L* branches. The amplitude of the action potentials in the parent axon, *Ax* and the branch *M*, time to peak and rate of rise did not differ (Table 1).

Space constant and membrane resistance. The equations relating the space constant and input resistance for infinite cables were used. (Hodgkin & Rushton, 1946; Papir, 1973). The micro-electrodes were inserted into Ax several mm (5–7) before the bifurcation so that the axon could be approximated by an infinite cylinder. Three micro-electrodes were inserted into the Ax region. Each electrode recorded the

TABLE 1. Resting potential (RP) and action potential (AP) characteristics in Ax and M. Results given as mean ± standard deviation. Number of measurements are given in parentheses

	RP (mV)	AP amplitude (mV)	AP rise time (msec)	AP rate of rise (V/sec)	Threshold (mV)	Refractory period
Ax	65·0 ± 4·2 (15)	96·1 ± 11·4 (17)	0·55 ± 0·17 (16)	421 ± 170 (16)	18·6 ± 1·7 (5)	2·84 ± 1·11 (5)
M	65·6 ± 4·6 (15)	92·1 ± 13·2 (17)	0·65 ± 0·17 (14)	360 ± 144 (15)	23·5 ± 4·5 (10)	4·0 (2)

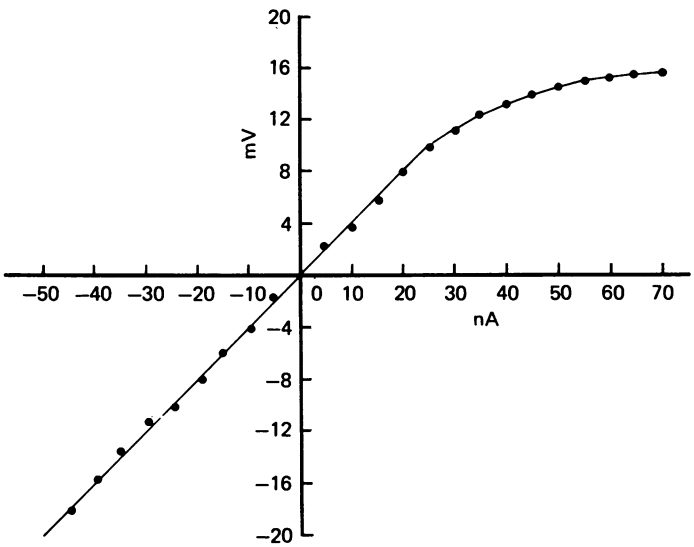

Fig. 3. Current–voltage curve for the common excitatory axon. Two micro-electrodes 200 μm apart were inserted into the Ax region. One served for passing of current (square pulses), the second recorded the membrane potential drop. Note rectification at about 10 mV depolarization.

membrane potential and each in turn served for passing current into the axon. From the decay of the membrane voltage drop (in the hyperpolarized direction) with distance, the space constant was calculated. The current–voltage relation of the membrane was found to be linear in the range of -20 to $+8$ mV (Fig. 3) deviations from resting potential. For depolarizations above 10 mV, strong delayed rectification was seen. The slope of the current–voltage curve for each distance between electrodes was measured in the linear range. The values obtained were plotted against distance giving a straight line that could be extrapolated to zero distance to give the input resistance. From the input resistance and the space constant the specific membrane resistance (R_m) and specific internal resistance (R_i) were computed. The time constant

τ was calculated as described by Papir (1973). The results obtained for four axons are given in Table 2.

Conduction block at high frequency. The development of a conduction failure from Ax into M and L during high frequency stimulation is demonstrated in the experiment of Fig. 4. Furthermore, this experiment shows that conduction block appeared after

TABLE 2. The membrane electrical properties of the common excitatory axon

No.	d(μm)	Input resistance (kΩ)	τ_m (msec)	λ(μm)	R_i(Ω cm)	R_m(Ω cm^2)	c_m (μF/cm^2)
1	60	200	1·3	1090	104	822	1·5
2	70	240	1·2	1060	174	1119	1·0
3	75	320	2·0	1220	232	1804	1·0
4	65	295	1·8	1020	192	1228	1·4

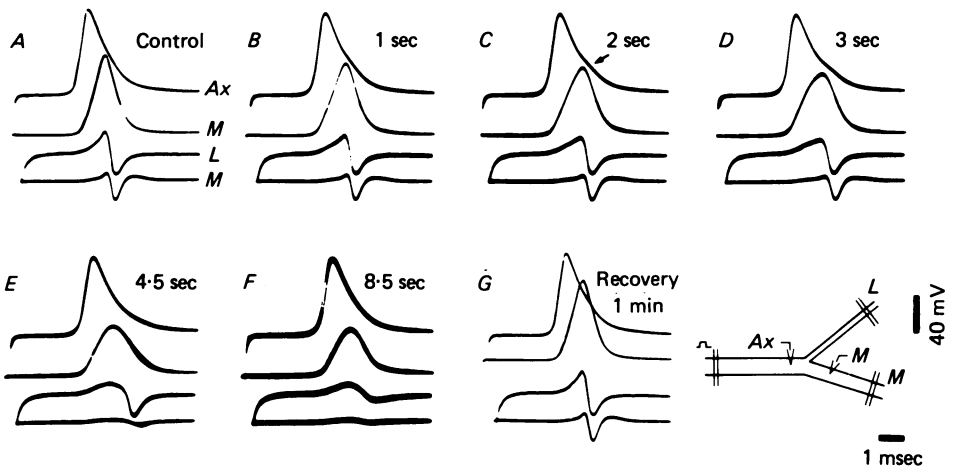

Fig. 4. Differential conduction block at the M and L branches. The experimental setup is given in the inset. Top two traces intracellular recording at Ax and M. Bottom two traces extracellular recording at M and L 3 mm after the branch point. *A*, control; note slower rise time in the M action potential. *B*, *F* stimulation at 50 Hz at Ax. Time of stimulation indicated above traces. Exposures composed of five superimposed sweeps. *C*, after 2 sec of stimulation; note hump (arrow) on falling phase of Ax action potential. *E*, when conduction into M was blocked the hump on the falling phase of the Ax action potential was missing. *F*, conduction block in both the M and L branches. *G*, recovery after rest.

different times in the M and L branches. Intracellular records were made from Ax and M about 200 μm proximal and distal to the bifurcation (Fig. 4*A*, Ax, M, upper traces). In addition action potentials were monitored extracellularly 3 mm distally to the bifurcation in the M and L branches (M, L lower traces and see inset in Fig. 4). At a low frequency (1 Hz) of stimulation (Fig. 4*A*), the Ax action potential propagated into both the M and L branches showing a slightly slower rise time in M. During 4 sec of stimulation at 50 Hz a progressive reduction in the amplitude of Ax and M action potentials was observed (Fig. 4*B–D* and Fig. 5). When the Ax action potential was reduced by 9 % of its original value, a potential of 50 mV was recorded in the M

branch. As evidenced from the extracellular recording, this 50 mV potential was below threshold to initiate a propagated action potential (Fig. 4*E*, lower trace). At this stage the *L* branch continued to conduct action potentials as can be seen from the response at the extracellular electrode. However, after 8·5 sec of stimulation, the *Ax* action

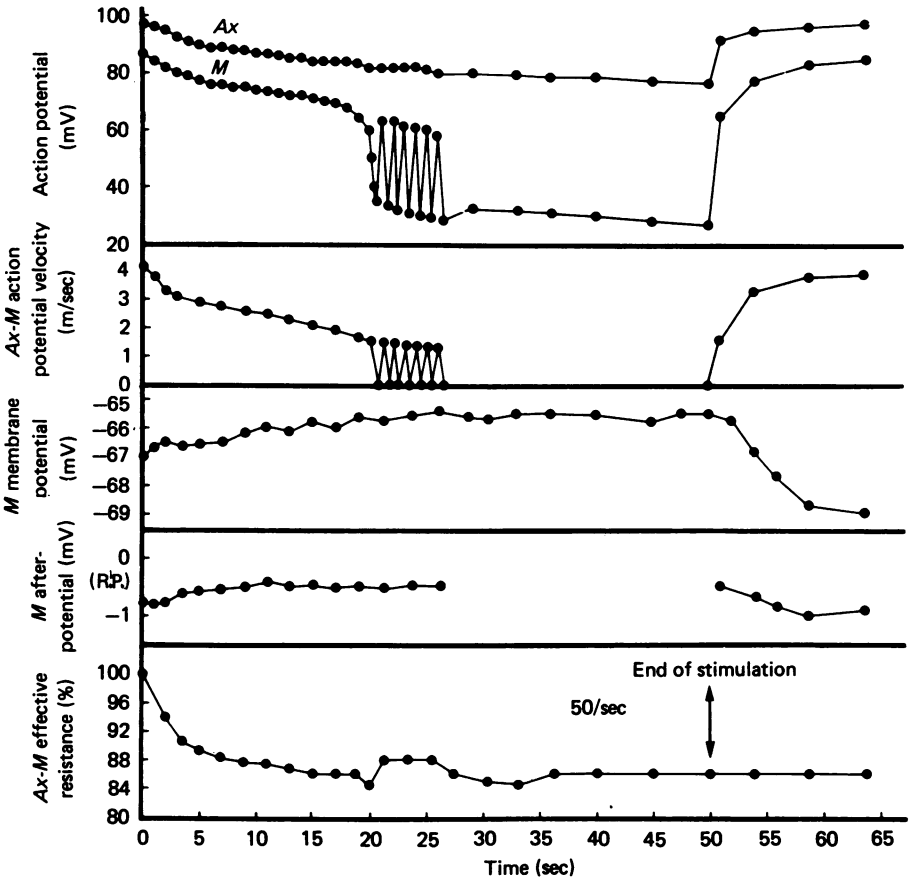

Fig. 5. Changes in action potential amplitude, conduction velocity, after-hyperpolarization and effective membrane resistance in *Ax* and *M* during and after 50 Hz stimulation. The data were obtained from pictures taken at a rate of 1/sec. Each exposure was composed of five superimposed sweeps. Experimental setup was the same as in Fig. 4. Conduction velocity was measured between the *Ax* and *M* recording sites. Effective membrane resistance was computed from the membrane potential drop after a square pulse of current given by the *Ax* micro-electrode. The afterhyperpolarization is given as deviation from resting potential.

potential was further reduced (12 %), and conduction along the *L* branch was blocked as well (Fig. 4*F*). After conduction was blocked in both branches, a depolarizing potential of 45 mV was recorded at *M* in response to *Ax* stimulation (Fig. 4*F*). Such a depolarization at the onset of the experiment was above threshold for the initiation of an action potential (see also Table 2) and thus we conclude that the threshold of the *M* branch was increased during the repetitive activation. After a short period of rest (seconds), conduction of single action potentials was seen in both branches (Fig.

4*G*). Complete recovery as judged by the time required to produce a block at 50 Hz occurred only after 20 min of rest.

Some other changes in the shape of the action potentials during repetitive firing are noteworthy. During high frequency stimulation the rise time of the *M* action potential became longer (Fig. 4*A–D*, second trace) and the delayed peak of the *M* action potential was reflected as a hump on the falling phase of the *Ax* action potential (Fig. 4*C*, arrow, and *D*). In Fig. 4*E*, where the response recorded in *M* was due to passive current spread (as evidenced by the lack of conduction) the hump on the falling phase of the *Ax* action potential was missing. Reflexion potentials from branch *L* into *Ax* and *M*, which are not prominent in this Figure, will be discussed later (see Fig 12).

A quantitative analysis of the changes occurring in the shape of the action potential, conduction velocity, membrane potential and effective membrane resistance during stimulation at 50 Hz is given, for another experiment in Fig. 5. The main points to observe are these. When *Ax* action potential amplitude was reduced by about 15 % intermittent conduction was seen in branch *M*. Although little further reduction in *Ax* action potential amplitude was observed, conduction in the *M* branch became slower and eventually was blocked. The change in resting potential in the *M* branch was small, about 1·5 m*V* depolarization. During repetitive firing, the membrane resistance was reduced by about 13–15 %; such a change could not have resulted from the small membrane depolarization seen and delayed rectification (Fig. 3).

These results clearly show that conduction block can occur at a branch point even in cases where the geometrical ratio is one. Thus, other factors, depending on activity of the axon, are involved in the development of the conduction block.

Effects of the geometrical ratio on conduction block at high frequency. The isolated axon is a convenient model for the study of the effects of geometrical factors on conduction block at high frequency. While in the orthodromic direction (*Ax* to *M* and *L*) the geometrical ratio of Rall (1959, 1964) is about one, in the same axon in the antidromic direction (*M* to *Ax* and *L*) the geometrical ratio is about 1·3. Thus in the first case, propagation of the action potential from *Ax* to *M* and *L* is equivalent to propagation into an axon of the same diameter as *Ax*. In the second, it is equivalent to propagation of an action potential through a region with a step increase in axon diameter (Goldstein & Rall, 1974).

In order to demonstrate the contribution of the dimensional factor, the responses of *Ax* and *M* were compared at various frequencies for orthodromic and antidromic stimulation. Fig. 6 shows the change in amplitude of the post-bifurcation action potentials at different frequencies for orthodromic (*A*) and antidromic (*B*) (in this experiment the geometrical ratio = 1·4) stimulation. In general, the conduction in the antidromic direction at high frequency is more vulnerable and a smaller number of action potentials at a given frequency or a lower frequency of stimulation is required to induce the conduction block than in the orthodromic direction. Thus, although the geometrical ratio by itself is not sufficient to explain the differential conduction block, it still has an effect on the rate at which the conduction block develops at the bifurcation.

Site of conduction block. The orthodromic-antidromic experiment showed not only that conduction across the bifurcation region is more vulnerable in the antidromic

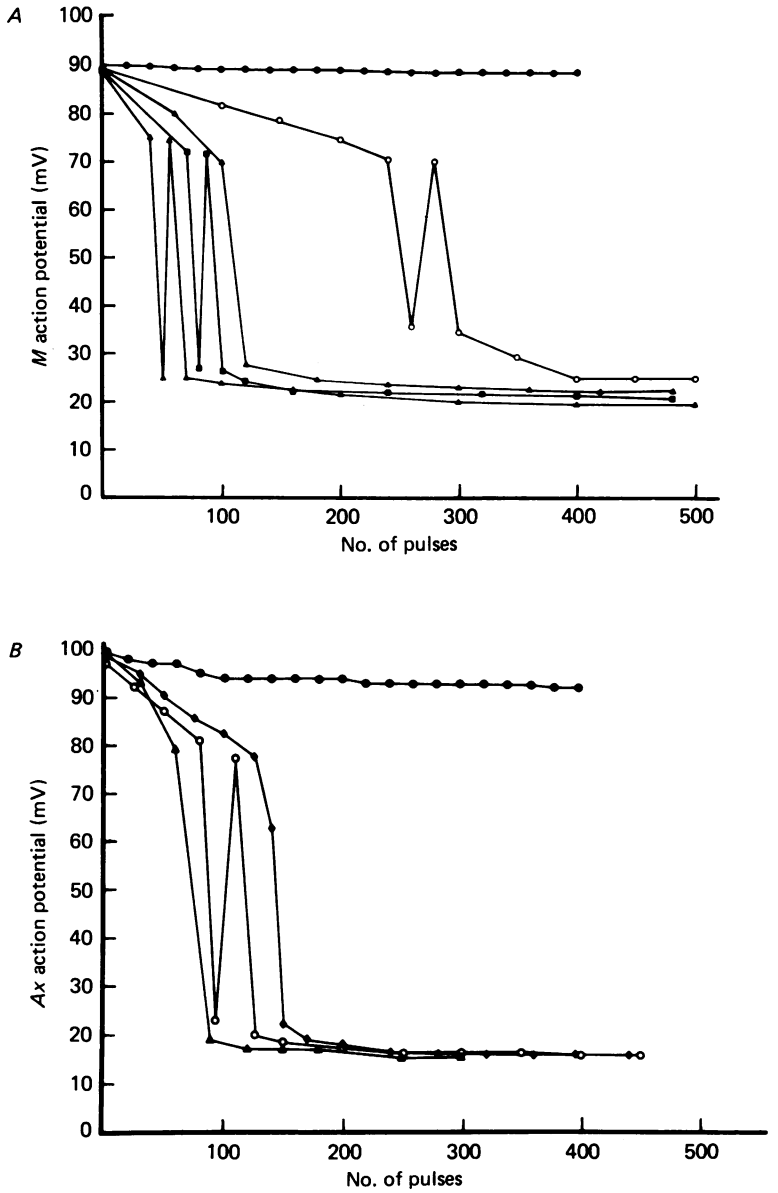

Fig. 6. Effect of the geometrical ratio on conduction of action potentials at different stimulation frequencies. *A*, orthodromic conduction from *Ax* into *M* and *L*, *GR* = 1. Orthodromic stimulation: ●, 10/sec; ○, 50/sec; ▲, 60/sec; ■, 80/sec; △, 100/sec. *B*, antidromic conduction from *M* into *Ax* and *L*, *GR* = 1·4. Antidromic stimulation: ●, 10/sec; ◆, 40/sec; ○, 50/sec; ▲, 60/sec.

direction as expected from geometrical considerations, but more importantly that the block of conduction occurs at the bifurcation region *per se*. We arrive at this conclusion from the following experiment (Fig. 7). Two micro-electrodes were inserted into the axon, one at *Ax* and the second at *M*. Each branch was stimulated with extracellular electrodes at 50 Hz; in one series stimulation at *Ax* (orthodromic) was first (*A–C*)

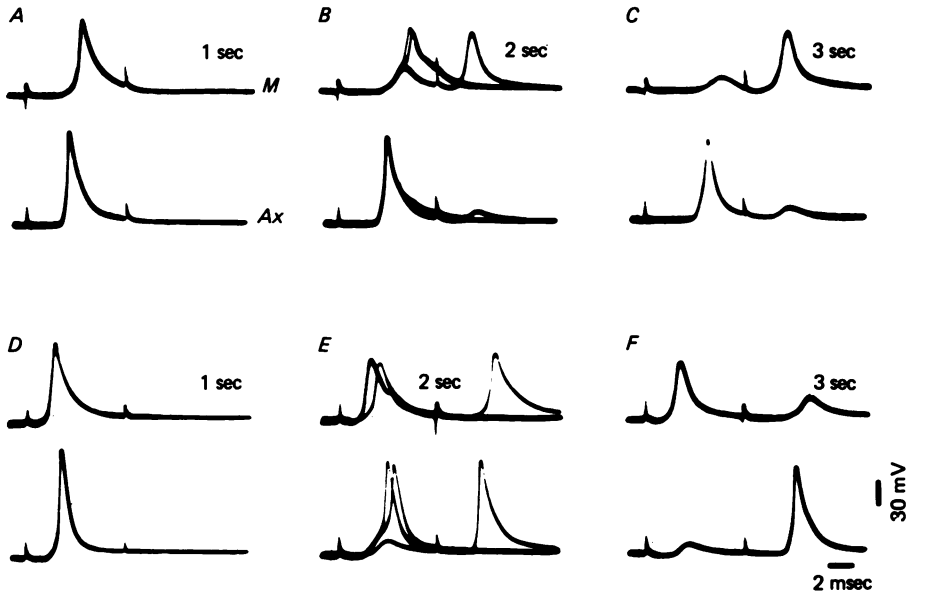

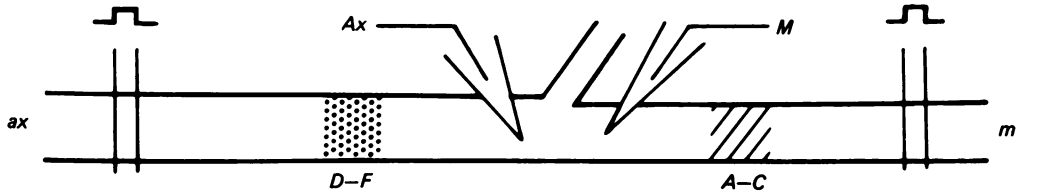

Fig. 7. Collision experiment showing that conduction block at high frequency occurs at the branch point. The experimental setup is shown in the inset. The axon was stimulated with extracellular electrodes both at *Ax* and *M*. In the first series (*A–C*) *Ax* stimulation preceded *M* stimulation by 8 msec, such that the orthodromic and antidromic action potentials collided distally to the *M* micro-electrode (diagonal bars). Therefore, in the control *A*, the two micro-electrodes *Ax* and *M* recorded only the orthodromic action potential. *B*, after 2 sec of stimulation at 50 Hz the action potential failed to invade from *Ax* into *M* and at the same instant, the *M* electrode recorded the antidromic potential (upper beam right) which failed to invade into the *Ax* region. In *B*, superimposed sweeps. *C*, same as B. *D–F*, in this series *M* stimulation preceded that of *Ax*, such that collision occurred at a point proximal to the *Ax* micro-electrode (dots in inset). *D*, control, *Ax* and *M* recorded only the antidromic potentials. *E*, after two seconds of stimulation at 50 Hz conduction from *M* into *Ax* was blocked (lower beam left), but at this instant *both* micro-electrodes recorded the orthodromic potential. Compare *B* and *E*. *F*, 1 sec later conduction from *Ax* to *M* was also blocked.

and in the second *M* stimulation (antidromic) was first (*D–F*). In Fig. 7*A–C*, the orthodromic stimulation precedes the antidromic stimulation by 8 msec. With this time interval, orthodromic action potentials were recorded in both branches; antidromic action potentials were not recorded in either *M* or *Ax* (Fig. 7*A*). This result indicates that collision of the orthodromic and antidromic action potentials had occurred somewhere in branch *M*, distal to the intracellular *M* micro-electrode. As

soon as the orthodromic action potential failed to invade the M branch (Fig. 7B) (and therefore collision could not occur), an antidromic action potential was recorded in M but not in Ax. This result clearly shows that when Ax-M transmission was blocked, the M branch could still conduct action potentials. The antidromic action potential, however, did not propagate into the Ax region (Fig. 7 B, C, lower trace),

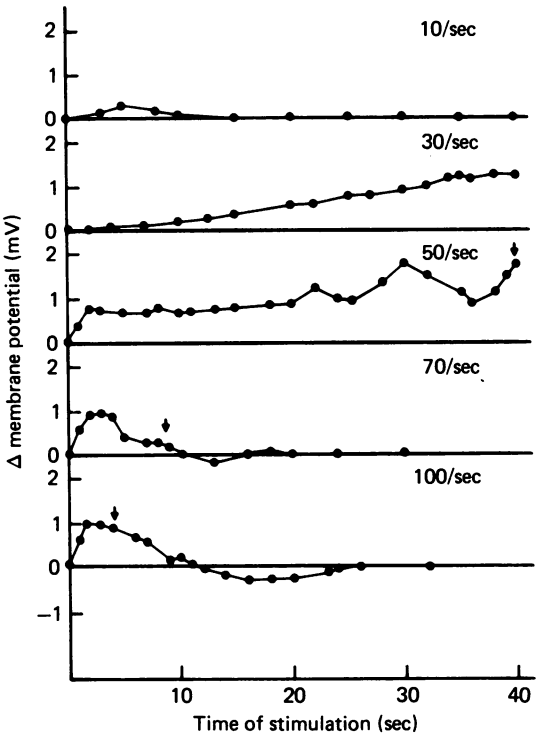

Fig. 8. Changes in membrane potential with time at different rates of stimulation. The axon was stimulated at Ax and action potentials recorded intracellularly at M. Arrows point the time of conduction block at each frequency.

and only a small potential was recorded in Ax. This antidromic action potential could not bring the Ax region to threshold because the changes occurring during high frequency activation leading to a conduction block for orthodromic impulses were sufficient to block antidromic conduction as well.

In Fig. 7D–F, the antidromic impulse preceded the orthodromic. In the control (Fig. 7D) only the antidromic action potential was recorded in the two branches and collision took place proximally to the Ax micro-electrode. After stimulation at 50 Hz, the antidromic action potential failed to invade Ax (Fig. 7E, lower trace) but now the orthodromic action potential was recorded *both* in Ax and M (compare with 7B). This result demonstrates that the changes occurring during 50 Hz stimulation sufficient to produce M to Ax block (GR = 1·4) were insufficient to produce Ax to M conduction block (GR = 1), and demonstrated again the contribution of the geometrical ratio to block of conduction at high frequency. However, one second later orthodromic conduction was blocked as well (Fig. 7F). Again, the results presented in Fig. 7D–F,

clearly show that when *M* to *Ax* conduction was blocked, the entire *M* branch could still conduct action potentials.

Changes in resting potential. The geometrical ratio of the axon, although contributing to the rate at which conduction block appeared (when the ratio was greater than 1) could not account for the differential appearance of the block at the two branches (Parnas & Segev, 1979). Factors such as membrane depolarization which in the cockroach axon could account for a conduction block (Spira *et al.* 1976), might be also of importance here. However, we found that during high frequency stimulation the membrane depolarized by only 1–3 mV (Fig. 5) when conduction at 50 Hz into the *M* branch was blocked. In Fig. 8, changes in resting potential during stimulation at different frequencies are shown. At the higher frequencies studied (70–100 Hz), the membrane did not show persistent depolarization but underwent hyperpolarization starting a few seconds after the onset of stimulation and continuing even after conduction block occurred (arrow, Fig. 8). The nature of this hyperpolarization is discussed in the following paper (Grossman *et al.* 1979). This experiment also shows that there is no correlation between the membrane depolarization and the time of the appearance of the conduction block into branch *M*. That the small depolarization seen after high frequency stimulation was not responsible for the conduction block can be deduced from experiments where the membrane was depolarized by intracellular outward current injection. Ten to twelve mV depolarizations for durations of 10–50 msec were insufficient to produce a conduction block for single action potentials. Stronger depolarizations, of 16–20 mV, were required to block conduction. The effect of a prolonged depolarization was also tested. Even 8 mV depolarization for 100 sec (amplitude and duration exceeding those obtained during repetitive stimulation) did not produce a conduction block. However, the depolarization did accelerate the development of conduction block after high frequency stimulation. For example, the time required to produce a conduction block at 50 Hz was shortened by 20 % when the membrane was depolarized by 10 mV during the stimulation period.

It is concluded that the depolarization seen during high frequency activation of an axon by itself is insufficient to produce the conduction block.

Changes in stimulation current intensity. The results described in the experiment of Fig. 7 show that conduction in the *M* branch persisted after *Ax-M* transmission was blocked. This suggests that the threshold for initiation of action potential along the *M* branch had increased, especially since potentials as high as 45 mV in amplitude, arriving from *Ax*, were insufficient to evoke a propagating action potential in *M*. In order to measure changes in threshold the axon was stimulated intracellularly at either *Ax* or *M* and the minimal current intensity (0·5 msec pulses) required to induce an action potential was measured. We found that after a few seconds of stimulation at 50 Hz (10 sec), a current pulse 4 times stronger than the control was needed in order to elicit an action potential.

Responsiveness to twin impulses. The absolute refractory period, as determined by direct intracellular stimulation, was about the same for *Ax* and *M* and it varied between 1·5 and 4 msec (Table 1). However, the time interval between a pair of action potentials in order that both would be conducted from *Ax* into *M* and *L* was found to be an order of magnitude longer, to vary greatly from preparation to preparation and to be different for the *M* and *L* branches. In the experiment described in Fig. 9, *Ax*

was stimulated with twin impulses with a varying time interval at a low repetition rate. Branch L was found to respond to the twin impulses in Ax at much shorter intervals than M (Fig. 9C) and in a few cases it responded with the shortest interval for Ax itself. Branch M always required long intervals for the second action potential to propagate from Ax. When branch M was stimulated directly, its refractory period was similar to that of Ax, in the range of 4 msec.

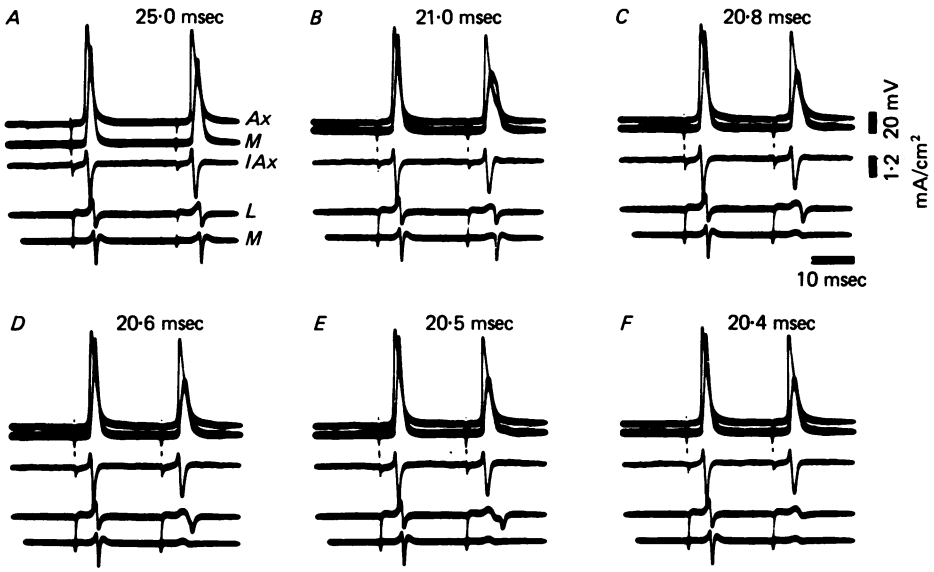

Fig. 9. M and L branch responsiveness to twin impulses given at Ax. Experimental setup same as in Fig. 4. In this experiment membrane current I_{Ax} was measured at Ax before the bifurcation. Interval between impulses given above traces. Note that conduction of the second impulses in M and L failed with different intervals (C, E).

Such a difference in the 'responsiveness' of the two branches to action potentials invading from Ax is reflected in their ability to conduct short high frequency action potential trains. Fig. 10 shows the responses to three impulses with varying intervals, given at Ax. It is clear that branch M can pass short trains of impulses only at the lower frequencies, while branch L can follow Ax at higher frequencies (Fig. 10C).

Difference in the responsiveness of the M branch in comparison to that of Ax can be demonstrated in another way (Fig. 11). Ax was stimulated repeatedly with three impulses 7 msec apart, at a repetition rate of 10 Hz. At first, three action potentials were recorded both at Ax and M (Fig. 11B–C). However, with time, changes occurred in the M responses while in Ax the three action potentials were always recorded (Fig. 11D–F). That block of conduction of action potentials from Ax to M can occur with short impulse trains separated by longer intervals suggests that the changes produced by the repetitive activation of the axon are cumulative. The time for complete recovery was much longer than the interval between the impulse trains (85 msec).

Changes in membrane current during repetitive activation. The changes seen in membrane voltage responses during and after high frequency activation are not sufficient to reveal the underlying ionic currents. For example, is the 45 mV depolari-

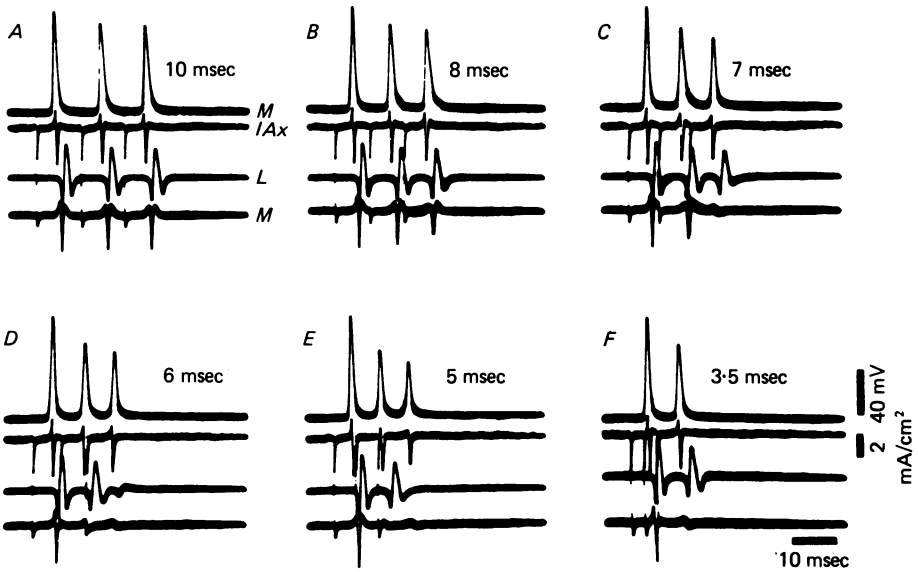

Fig. 10. Responsiveness of the M and L branches to three impulses evoked at Ax. Interval between impulses given above traces. M action potential was recorded intracellularly and M and L branch conduction recorded extracellularly. In this experiment conduction of Ax was measured with the patch clamp electrode (I_{Ax}). Note the differences in M and L responses while Ax conducted always the three action potentials.

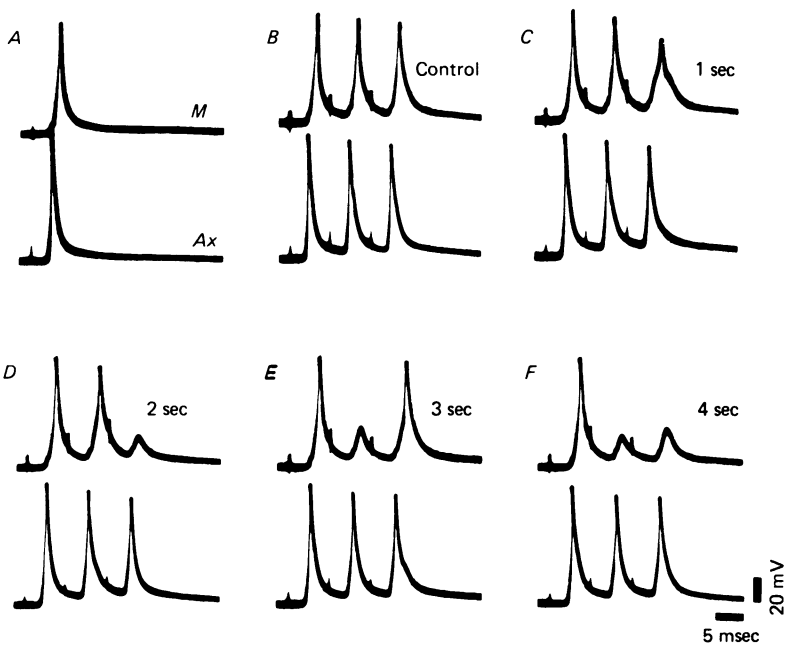

Fig. 11. Stimulation at Ax with a burst of three impulses (7 msec apart), bursts repeated at a frequency of 10 Hz. Action potentials recorded in M and Ax. A, control. B–F, time of stimulation given above traces. While Ax recorded always the three impulses, M responded only partially.

zing potential (see Fig. 4*E*, *F*) seen in the *M* branch after *Ax-M* conduction block due to reduced (partially inactivated) inward Na current at *M* or to spread of current from an active region in *Ax* flowing outward to produce membrane depolarization at *M*? Current measurements can distinguish between such possibilities. The method of intracellular voltage clamping (Hodgkin & Huxley, 1952) would have been ideal for

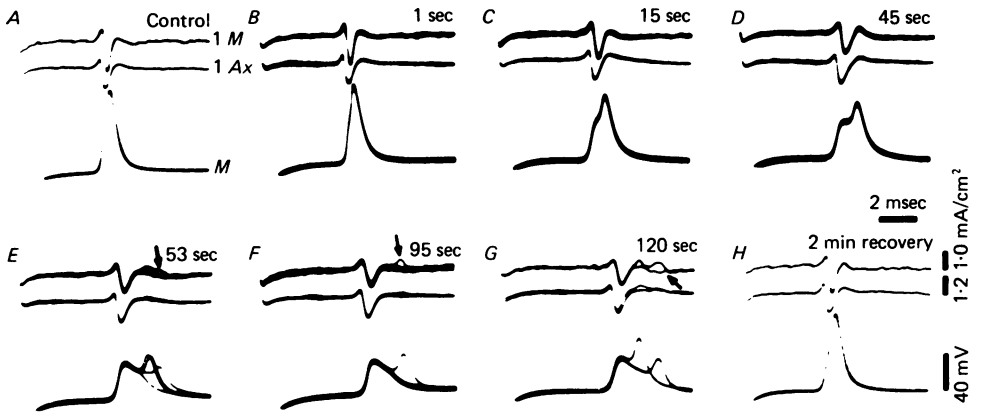

Fig. 12. Changes in membrane currents during stimulation at 25 Hz. The axon was stimulated at *Ax*, and action potentials recorded intracellularly at *M*. Membrane current was recorded with patch clamp at *Ax* and *M*. *A*, control, inward current density for *Ax* and *M* was 1·6 and 1·5 mA/cm² respectively. Note different current calibration for *Ax* and *M*. *B–G*, stimulation at 25 Hz, time of stimulation given above traces. In *F* arrows point to the delayed currents associated with the reflexion potentials (lowest beam). For further detail see text.

such current measurements. Unfortunately, in preliminary experiments we could not clamp the region of the bifurcation with two intracellular micro-electrodes because of current leaking through the long and open branches. We therefore use the patch clamp technique (Neher & Lux, 1969) which enabled measurement of membrane currents from small defined membrane areas at *Ax*, *M* and *L* branches just proximal and distal to the bifurcation.

The membrane current for a propagating action potential is triphasic (Noble, 1966, Fig. 12*A*). The first phase is positive and represents mainly capacitative current. The second phase is negative and consists mostly of inward ionic current. The third phase is positive and is partially produced by current spreading retrogradely from the next activated region during the refractory period at the point measured. We have measured the membrane current for single action potentials in *Ax*, *M* and *L* branches. The maximal inward current varied in the different preparations (24 axons) between 0·75 and 3 mA/cm². However, in the same axon the current density measured in *Ax*, *M* and *L* did not vary by more than 10 %.

It should be noted that the third phase of the membrane current is not always discernible in actual experiments (see, for example, Fig. 9*A*, or Fig. 2 in Grossman *et al.* 1979). In these cases, the biphasic response is fast with a large negative phase. The biphasic response is slower and smaller when the membrane potential change is passive (see also Parnas & Segev, Fig. 9).

Fig. 12 shows the changes that occur in the shape of the action potential and the membrane currents during repetitive activation. The stimulation rate at *Ax* was only

25 Hz, in order to produce the changes more distinctly over an extended period of time. In the control (Fig. 12*A*), the maximal inward current (measured from the base line) in *Ax* and *M* was 1·6 and 1·5 mA/cm² respectively. When *Ax* to *M* conduction was gradually blocked (Fig. 12*E–G*), the peak inward current was reduced in *M* by 40–45 % and only by 5–10 % in *Ax*. At this stage the current recorded in *M* was biphasic; the

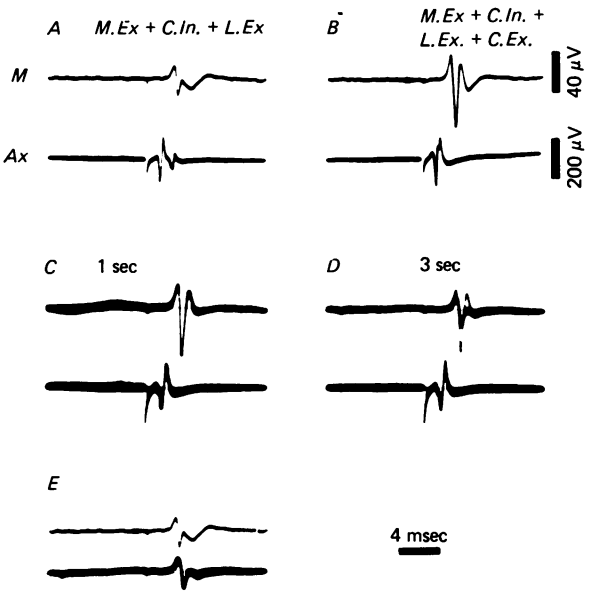

Fig. 13. Compound action potentials recorded from the nerve bundle innervating medial and lateral in the animal. Recording electrodes were placed around the *Ax* region and the *M* region (see Methods). Stimulating electrodes were placed more centrally also around the *Ax* region. *A*, the *Ax* and *M* responses after recruitment of the specific excitatory axon to *M*, *M.Ex*, the common inhibitor *C.In.* and the excitor to *L*, *L.Ex*. *B*, with further increase of stimulus intensity the common excitor was recruited. Note the change in *Ax* and *M* compound action potential. *C*, after 1 sec of stimulation at 50 Hz there was no change in either the *M* or *Ax* responses. *D* after 3 sec of stimulation there was a sudden drop of the response in *M* without a concurrent change in *Ax*. *E* comparison of the remaining *M* response in *D* (lower trace) with that of the control *A* before the recruitment of the common excitor (upper trace). Note the similarity between the two responses which indicates that the only missing component in the response was that of the common excitor.

third positive phase was missing. In addition the delayed depolarizing potentials recorded in *M* (Fig. 12*E–G*) were associated mainly with outward currents (arrows), indicating current spread from another region. However, since conduction in *M* was blocked, we may conclude that the delayed responses are produced by current spreading from the delayed action potentials at branch *L* (not recorded). With further repetitive stimulation those delayed depolarizing potentials in *M* disappeared, and their disappearance was associated with conduction block in *L* (not shown).

Chronic recording from the free-moving animal. The conditions required to produce a conduction block in the isolated bifurcating axon are either long-term stimulation (0·5 to several seconds) at 50–100 Hz (Fig. 6), or short (3–4 impulses) high-frequency trains repeating at a slower rate (10 Hz, Fig. 11). In order to claim that such 'frequency

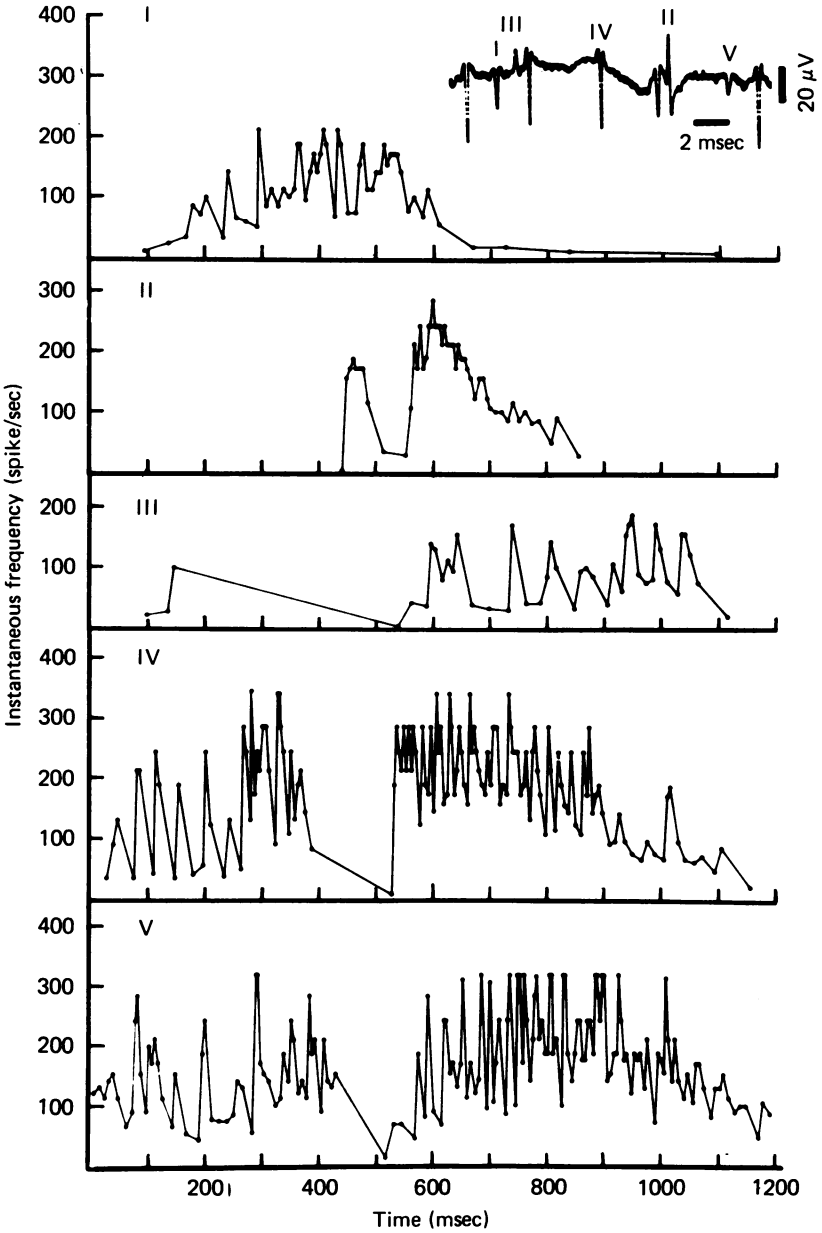

Fig. 14. Spontaneous activity of the five axons was recorded in the animal before the branching point region. A section showing activity of five units is shown in the inset. The frequency of each unit in one burst is given.

blocks' are physiological and not simply due to improper oxygen supply or unbalanced salt solution, it is necessary to demonstrate in an *in vivo* experiment that the same parent axon fires at frequencies at least as high or even higher than those used in our experiments, and to demonstrate differential conduction into the two branches. Accordingly, two electrode pairs were implanted around the main *Ax* branch (see Methods). The proximal was used for stimulation, the distal for recording (*Ax* in

Fig. 13*A*). Recording electrodes were placed also around branch *M* (*M* in Fig. 13*A*). The *L* branch is too small to record directly from it. *Ax* was stimulated with gradually increasing intensities to recruit the different axons (1–5, Parnas & Atwood, 1966). The identity of each axon was inferred from simultaneous recording of *Ax* and *M* activity and myograms from both the medial and lateral bundles of the deep abdominal muscles (myograms not shown). In the experiment described in Fig. 13, the common excitor axon, innervating the medial and lateral branches, was recruited last (compare Fig. 13*A* and *B*). Stimulation at *Ax* at 50 Hz for 3 sec produced a *sudden* diminution in the M compound action potential. At that time (and even later) no change was seen in the *Ax* response (compare Fig. 13*C* and *D*). The *M* response in Fig. 13*D* (after the sudden drop in amplitude) is similar to that in Fig. 13*A* (before the recruitment of the common excitor axon, see Fig. 13*E*). This result indicates block of conduction in the common excitor axon. We thus know that conduction block after high frequency stimulation can occur in the animal.

To determine whether these axons (at least the common excitor) fire at high frequency for a sufficient length of time in the animal to cause block, one pair of recording electrodes was placed around the main *Ax* bundle and the ongoing nervous activity was recorded while the animal was swimming. The signal to noise ratio made it possible to discriminate five distinct action potentials (Fig. 14, inset). Since in this experiment (one of twelve), we did not record the muscle activity we cannot attribute each action potential shape to a given axon. The action potentials are therefore marked I to V to indicate different axons. In the free moving animal the activity in the five units appeared in bursts, each burst lasting for a few hundred msec. Fig. 14 shows the instantaneous frequency of the action potentials in one example of a burst lasting 1·2 sec. The peak frequencies for the different units varied from about 150–350 Hz (in other experiments the frequency varied between 100 and 400 Hz) and all units had periods of 300 msec or longer during which the mean frequency exceeded 100 Hz. As shown above, such a frequency range is often sufficient to produce a conduction block into branch *M* in the isolated preparation. However, in three experiments where we have recorded spontaneous axonal activity both at the *Ax* and *M* branch, we could not establish a clear case of a conduction block across the bifurcation.

DISCUSSION

The phenomena of conduction block and differential channelling of action potentials at branch points of an axon have by now been shown to occur in several preparations (Barron & Matthews, 1939; Tauc & Hughes, 1963; Kennedy & Mellon, 1964; Chung *et al.* 1970; Van Essen, 1973, Yau, 1976). However, they were never demonstrated before by direct measurement at a branch point, *per se*. In the present study the common excitatory axon innervating the medial and lateral muscle branches was used to observe directly the changes occurring at the bifurcation during high frequency activation. The conduction block does not seem to be an artifact of the experimental condition of the isolated preparations since it could be produced by stimulation of the nerve *in situ* in the moving animal, where nerves are under constant flow of blood and unimpaired oxygen supply (Krnjević & Miledi, 1959).

During high frequency activation (both orthodromically and antidromically) the

amplitude of the action potential was reduced over the whole length of the axon. However, conduction was blocked only in the bifurcation region. Moreover, the conduction block appeared at *different* rates in the two branches. Such a result calls for an extension of the Rall (1959, 1964) and Goldstein & Rall (1974) models for the propagation of action potentials in branching axons. These models suggest that conduction of an action potential from a main axonal branch into its daughter branches depends only on the geometrical ratio if the membrane properties of all branches are the same.

For the case of the common excitatory axon the geometrical ratio

$$GR = \frac{d_M^{3/2} + d_L^{3/2}}{d_{Ax}^{3/2}}$$

(where d_M, d_L and d_{Ax} are the diameters of the daughter and main branch respectively) is one. In this case propagation into the two branches should be equal and independent of branch diameter. The safety factor for propagation of action potentials into the branches should be the same as that for the conduction of an action potential into an equivalent axon of the same diameter as that of the main branch. In branching axons where the geometrical ratio is greater than one, conduction is equivalent to the case of a step increase in axon diameter. As the geometrical ratio is increased, or excitability is reduced, conduction should fail in *both* branches at the *same* time (Goldstein & Rall, 1974; Parnas & Segev, 1979).

In the common excitatory axon ($GR = 1$) single action potentials propagate into the two branches. At high frequency, however, conduction failed first into *one* branch only and later in the other. The latter finding implies that development of impedance mismatching by local changes in conductance does not seem to be the cause for the *dynamic changes* observed during high frequency activation.

An attempt to explain differential channelling of action potentials in a branching axon was made by Zeevi (1972, and personal communication). He postulates in his theoretical computations different maximal sodium conductances for the two branches. However, such a difference was not demonstrated experimentally either by Zeevi or by others. On the contrary, from the limited data we have, it seems that the main branches (Ax, M, L) of lobster axons have the same inward membrane current densities. In addition, the comparison of action potential shape and membrane currents (amplitude, rise time, etc.) in the Ax and M branches (where it was possible to record intracellularly) shows no significant differences (Table 1). We will, therefore, attempt to explain the differential conduction block seen after high frequency stimulation by assuming that the cable properties and the sodium conductance (Hodgkin & Huxley, 1952) of the two branches are the same (see also Parnas & Segev, 1979).

The reduction in action potential amplitude (about 10 %) seen after high-frequency stimulation was associated with a 10–20 % decrease in effective membrane resistance and a small membrane depolarization of 1–3 mV. The small membrane depolarization, however, as tested by current injections, was not sufficient to account for the reduction in action potential amplitude and change in resistance.

Julian, Moore & Goldman (1962) showed that the ionic mechanisms involved in the production of the action potential in the lobster are similar to those in the squid (Hodgkin & Huxley, 1952). One possibility to consider therefore is that during high-

frequency activation intracellular Na concentration increases, leading to a decreased driving force for Na currents. However, if Na ions (about 10^{-12} mole/cm^2) flow into the cell with each spike (Frankenhaeuser & Hodgkin, 1956) and the diameter of the axon is taken as 50 μm, then disregarding any recovery processes, the change in Na concentration could only be about 1 mM after 1000 action potentials. The intracellular Na concentration in the lobster axon is 71 mM (Katz & Freeman, 1972) and addition of 1 mM will not affect the driving force appreciably. Therefore, changes in intracellular Na concentration cannot account for the reduction in the amplitude of the action potential during the high frequency activation.

The changes seen in the 'electrical responsiveness' of the axon, including slowing of the action potential rise time, increase in threshold, slowing of conduction velocity and prolongation of the refractory period all suggest a reduction in membrane excitability which could be explained by inactivation of the Na system. In the cockroach (Spira *et al.* 1976), high frequency stimulation produced 15–20 mV depolarization which is sufficient to produce sodium inactivation and conduction block. In the lobster, however, the depolarization observed after high frequency activation is too small to account for the changes seen. Other mechanisms such as effects of changes in intracellular and extracellular ionic concentrations on membrane excitability must be considered (Jansen & Nicholls, 1973; Grossman *et al.* 1979).

The changes observed in membrane currents during repetitive activation can explain the nature of some of the changes seen in the action potentials (e.g. delayed potentials and reflexion potentials) (Khodorov *et al.* 1971; Parnas & Segev, 1979). Membrane current I_m is composed of three components:

$$I_m = C_m \frac{dv}{dt} + I_{ionic} + \frac{V}{R_m},$$

where the capacitative component $C_m\, dv/dt$ is proportional to the first derivative of the membrane potential and, therefore, is biphasic. V/R_m is the leakage current and is small compared to the capacitative and specific ionic currents. In an homogeneous axon, assuming a constant velocity (Hodgkin & Huxley, 1952), the membrane current is

$$I_m = \frac{a}{2R_i\theta^2} \cdot \frac{d^2V}{dt^2},$$

where a = radius of the axon, R_i the specific internal resistance and θ the conduction velocity. Thus, the membrane current is proportional to the second derivative of the voltage and is triphasic. In the case of an inexcitable membrane, an action potential spreading electrotonically from an active region will only generate capacitative current; the current record, therefore, should be biphasic (Noble, 1966). The currents associated with the delayed potential response (see, for example, Fig. 12*G*) were always biphasic (but see small print on p. 298) and, thus, we can conclude that the *M* membrane was not excited at those times. The delayed potentials seen in *M* must have spread electrotonically from the *L* branch which remained excitable and indeed they disappeared as conduction into *L* branch was blocked.

During repetitive stimulation, the current records in the region of the bifurcation became more complicated. Currents of the delayed action potential in the *M* and *L*

branches spread back to form 'reflexion potentials' in *Ax*. At the stage when conduction was blocked in *M*, the action potentials in *L* probably appeared after a longer delay to produce 'reflexion potentials' on top of the *M* electronic potentials spreading from *Ax*.

While in the present study we mainly used lobster axon as a model system to study the phenomenon of conduction block at branch point, it was of great interest to investigate whether such differential channelling of action potentials can be of physiological importance. The medial and lateral bundles of the nerve are synergistic muscles with different mechanical properties (Parnas & Atwood, 1966; Atwood, 1967). Both muscles are innervated by specific excitatory axons, as well as by a common excitatory and a common inhibitory axon (Parnas & Atwood, 1966). The animal can therefore, activate each muscle separately, by central control. We were unable to demonstrate, directly, that differential control of the two muscles is achieved by 'frequency filtering'. We showed, however, that conduction block at high frequency (50 Hz) could be produced by stimulating the axon in the free-moving animal, and that the axons in the animal fire at frequencies (100–400 Hz) sufficient to produce a block of conduction after a few impulses.

Recent studies by J. Wine (personal communication) show that during the escape response in the crayfish both the medial and lateral muscles exhibit synchronous activity for a few strokes after which activity abruptly stops in the medial muscle and continues in the lateral. However in this study no correlation between muscle myograms and the different axons (specific or common) has been established.

We are most grateful to Professor J. Dudel for his helpful discussions, for giving us the voltage clamp amplifiers and for letting Dr Grossman work in his laboratory to do part of the voltage clamp experiments. We are also grateful to Dr B. Wallace for critical reading of the manuscript. Supported by grant 741 from the Binational Science Foundation and by grant Az 11 1955 from Stiftung Volkswagenwerk.

REFERENCES

ATWOOD, H. L. (1967). Crustacean neuromuscular mechanism. *Am. Zool.* **7**, 527–551.

BARRON, D. H. & MATTHEWS, B. H. C. (1939). Intermittent conduction in the spinal cord. *J. Physiol.* **85**, 73–103.

BITTNER, G. D. (1968). Differentiation of nerve terminals in the crayfish opener muscle and its functional significance. *J. gen. Physiol.* **51**, 731–758.

CHUNG, S., RAYMOND, S. A. & LETTVIN, J. Y. (1970). Multiple meaning in single visual units. *Brain, Behav. & Evol.* **3**, 72–101.

FRANK, K. & TAUC, L. (1963). Voltage-clamp studies of molluscan neuron membrane properties. In *The Cellular Function of Membrane Transport*, ed. HOFFMAN, J. Englewood Cliffs, New Jersey: Prentice Hall, Inc.

FRANKENHAEUSER, B. & HODGKIN, A. L. (1956). The after-effects of impulses in the giant nerve fiber of Loligo. *J. Physiol.* **131**, 341–376.

GOLDSTEIN, S. S. & RALL, W. (1974). Changes of action potential shape and velocity for changing core conductor geometry. *Biophys. J.* **14**, 731–757.

GROSSMAN, Y., SPIRA, M. E. & PARNAS, I. (1973). Differential flow of information into branches of a single axon. *Brain Res.* **64**, 379–386.

GROSSMAN, Y., PARNAS, I. & SPIRA, M. E. (1979). Ionic mechanisms involved in differential conduction of action potentials at high frequency in a branching axon. *J. Physiol.* **295**, 307–322.

HATT, H. & SMITH, D. O. (1975). Axon conduction block: differential channelling of nerve impulses in the crayfish. *Brain Res.* **87**, 85–88.

HATT, H. & SMITH, D. O. (1976). Synaptic depression related to presynaptic conduction block. *J. Physiol.* **259**, 367–393.

HODGKIN, A. L. & HUXLEY, A. (1952). A quantitative description of membrane current and its application to conduction and excitation in nerve. *J. Physiol.* **117**, 500–554.

HODGKIN, A. L. & RUSHTON, W. A. H. (1946). The electrical constants of a crustacean nerve fibre. *Proc. R. Soc.* B **133**, 444–479.

JANSEN, J. K. S. & NICHOLLS, J. G. (1973). Conductance changes and electrogenic pumps and the hyperpolarization of leech neurones following impulses. *J. Physiol.* **229**, 635–655.

JULIAN, F. J., MOORE, J. W. & GOLDMAN, D. E. (1962). Current-voltage relations in the lobster giant axon membrane under voltage clamp conditions. *J. gen. Physiol.* **45**, 1217–1238.

KATZ, G. M. & FREEMAN, A. R. (1972). The scatter of intracellular ionic concentration in the lobster circumoesophageal axon. *J. comp. Physiol.* **81**, 89–98.

KENNEDY, D. & MELLON, D. (1964). Synaptic activation and receptive fields in crayfish interneurons. *Comp. Biochem. Physiol.* **13**, 275–300.

KHODOROV, B. I., TIMIN, YE. N., VILENKIN, S. YA. & GUL'KO, F. B. (1969). Theoretical analysis of the mechanisms of conduction of a nerve pulse over an inhomogeneous axon-I. Conduction through a portion with increased diameter. *Biofizika* **14**, 304–315.

KHODOROV, B. I., TIMIN, YE. N., POSIN, N. V. & SHEMELEV, L. A. (1971). Theoretical analysis of the mechanisms of conduction of nerve impulses over an inhomogeneous axon-IV. Conduction of a series of impulses through a portion of the fibre with increased diameter. *Biofizika* **16**, 95–102.

KRNJEVIĆ, K. & MILEDI, R. (1959). Presynaptic failure of neuromuscular propagation in rats. *J. Physiol.* **149**, 1–22.

NEHER, E. & LUX, H. D. (1969). Voltage clamp of *Helix pomatia* neuronal membrane: Current measurement over a limited area of soma surface. *Pflügers Arch.* **311**, 272–277.

NOBLE, D. (1966). Applications of Hodgkin–Huxley equations to excitable tissues. *Physiol. Rev.* **46**, 1–50.

PAPIR, D. (1973). The effect of glycerol treatment on crab muscle fibres. *J. Physiol.* **230**, 313–330.

PARNAS, I. (1972). Differential block at high frequency of branches of a single axon innervating two muscles. *J. Neurophysiol.* **35**, 903–914.

PARNAS, I. & ATWOOD, H. L. (1966). Phasic and tonic neuromuscular systems of the crayfish and rock lobster. *Comp. Biochem. Physiol.* **18**, 701–723.

PARNAS, I., HOCHSTEIN, S. & PARNAS, H. (1976). Theoretical analysis of parameters leading to frequency modulation along an inhomogeneous axon. *J. Neurophysiol.* **39**, 909–923.

PARNAS, I. & SEGEV, I. (1979). A mathematical model for conduction of action potentials along bifurcating axons. *J. Physiol.* **295**, 323–343.

RALL, W. (1959). Branching dendritic trees and motorneuron membrane resistivity. *Expl Neurol.* **1**, 491–527.

RALL, W. (1964). Theoretical significance of dendritic trees for neural input–output relations. In *Neural Theory and Modeling*, ed. REISS, R. F., pp. 73–97. Palo Alto: Stanford University Press.

RAMON, F., JOYNER, R. W. & MOORE, J. W. (1975). Propagation of action potentials in inhomogeneous axon regions. *Fedn Proc.* **34**, 1357–1365.

SPIRA, M. E., YAROM, Y. & PARNAS, I. (1976). Modulation of spike frequency by regions of special axonal geometry and by synaptic inputs. *J. Neurophysiol.* **36**, 882–899.

TAUC, L. & HUGHES, G. M. (1963). Modes of initiation and propagation of spikes in the branching axons of molluscan central neurons. *J. gen. Physiol.* **46**, 533–549.

VAN ESSEN, D. C. (1973). The contribution of membrane hyperpolarization to adaptation and conduction block in sensory neurones of the leech. *J. Physiol.* **230**, 509–534.

WATANABE, A. & TAKEDA, K. (1963). The spread of excitation among neurons in the heart ganglion of the stomatopod *squilla oratoria*. *J. gen. Physiol.* **46**, 773–801.

WAXMAN, S. G. (1972). Regional differentiation of the axons. Review with special reference to the concept of the multiples neuron. *Brain Res.* **47**, 269–288.

WAXMAN, S. G. (1975). Integrative properties of design principles of axons. *Int. Rev. Neurobiol.* **18**, 1–40.

YAU, KING-WAI (1976). Receptive fields, geometry and conduction block of sensory neurones in the central nervous system of the leech. *J. Physiol.* **263**, 513–538.

ZEEVI, Y. Y. (1972). Structural functional relationship in single neurons: SEM and Theoretical studies. Ph.D. Thesis, University of California, Berkeley, U.S.A.